Shape Changes of Statistical Copolymacromonomers: From Wormlike Cylinders to Horseshoe- and Meanderlike Structures

Tim Stephan, Sandra Muth, and Manfred Schmidt*

Institute of Physical Chemistry, Johannes Gutenberg University, 55099 Mainz, Germany

Received October 4, 2002
Revised Manuscript Received November 15, 2002

Introduction. Shape persistent cylindrical macromolecules of high directional persistence are of increasing interest because they may well serve as building blocks for the formation of well-defined macromolecular assemblies. Besides intrinsically stiff polymers or polymers with a helical superstructure, also flexible chains may exhibit a large directional persistence if densely decorated with linear or dendritic side chains.[1−12]

In such structures the intrinsically flexible main chain is stretched by the steric repulsion of the densely grafted side chains. The experimental results are in qualitative but not in quantitative agreement with recent computer simulations[13,14] which also predict an intramolecular phase separation to occur in statistical copolymacromonomers with incompatible side chains.[15]

In the present communication we describe the first experimental realization of statistical copolymer cylindrical brushes and provide evidence for intramolecular phase separation to occur, which results in shape variations of single macromolecules from wormlike to horseshoe or meanderlike structures.

Experimental Section. The PVP and PMMA macromonomers were prepared anionically and by GTP, respectively, as described elsewhere[7,9](see also Supporting Information). The molar mass characterization by MALDI−TOF and the degree of end-functionalization determined by NMR are given in Table 1.

Some MALDI−TOF and NMR spectra of the macromonomers are shown and discussed in the Supporting Information.

The sample code for the macromonomers consists of the end group (MA = methacrylate) followed by the abbreviation of the polymer (PVP or PMMA) and by the degree of polymerization P_n.

Both macromonomers were copolymerized to cylindrical copolymer brushes by free radical polymerization according to Scheme 1. It is important that the reaction mixture remains homogeneous during the polymerization.[16] The composition of the resulting copolymers as revealed by NMR is within experimental error identical to the monomer feed composition irrespective of conversion which represents strong evidence for a statistical copolymerization (see Table 2). For the copolymers the additional first number in the sample code gives the mean fraction of the respective macromonomer in weight percent. The characterization techniques (static and dynamic light scattering, AFM) are described in detail in the Supporting Information. To enhance the incompatibility between the side chains, both cylindrical copolymer brushes were quaternized by ethyl bromide (see Supporting Information). Sample 22PVP47-*co*-78PMMA35 was quaternized to 50%, yielding sample 22PVP47-*co*-78PMMA35-QEB50, and sample 73PVP47-*co*-27PMMA35 to 70%, yielding sample 73PVP47-*co*-27PMMA35-QEB70.

* Corresponding author: e-mail mschmidt@mail.uni-mainz.de.

Table 1. MALDI−TOF Characterization of the Macromonomers and Degree of End-Functionalization *f* Determined by NMR

macromonomer	M_n/g mol^{-1}	P_n	M_w/M_n	*f* (%)
MA-PVP47	5078	46.7	1.04	75
MA-PMMA35	3732	35.3	1.08	70

Scheme 1. Radical Copolymerization of Macromonomers

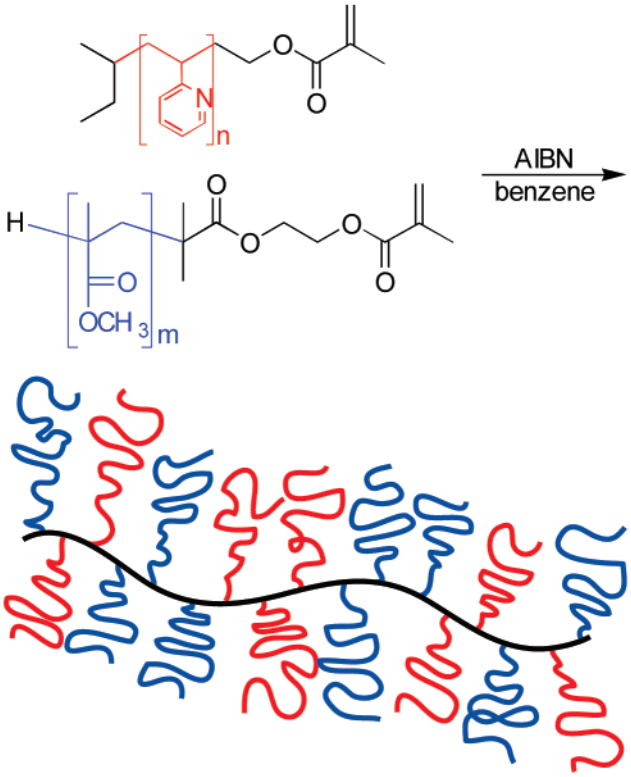

Results and Discussion. The neutral and the quaternized copolymer brushes were investigated by static and dynamic light scattering. The Zimm plots of the neutral copolymers are given in the Supporting Information. The resulting weight-average molar mass, the square root of the mean-square radius of gyration $\langle S^2\rangle_z^{1/2} = R_g$, and the reciprocal *z*-average of the inverse hydrodynamic radius $\langle 1/R_h\rangle^{-1} = R_h$ are given in Table 3. It is recognized that the dimensions of the cylindrical copolymer brushes hardly change upon quaternization. Because of the missing refractive increments d*n*/d*c*, the molar masses of the quaternized samples are not given in Table 3. However, with estimated values of d*n*/d*c* the molar masses correlate well with those calculated from the molar mass of the precursor polymers and the degree of quaternization. The results show that quaternization leads to somewhat larger radii of the copolymer brushes, thus excluding contraction of the quaternized polymers in those solvents from which they were spin-cast for AFM measurements, which are discussed below.

10.1021/ma025711r CCC: $22.00
Published on Web 12/04/2002

Table 2. Preparation and Composition (w/w) of the Copolymacromonomers

polymacromonomer	feed composition	conversion (%)	polymacromonomer composition
22PVP47-*co*-78PMMA35	79% PMMA35	50	78% PMMA35
	21% PVP47		22% PVP47
73PVP47-*co*-27PMMA35	30% PMMA35	26	27% PMMA35
	70% PVP47		73% PVP47

Table 3. Light Scattering Results of the Copolymacromonomers in DMF and AFM Results (L_w, L_n) of the Samples Spin-Cast from $CHCl_3$ Solution onto Mica

polymacromonomer	$M_w/10^6$ g mol^{-1}	R_g/nm	R_h/nm	L_w/nm	L_n/nm
22PVP47-*co*-78PMMA35	1.2	29.9	19.4	52	32
22PVP47-*co*-78PMMA35-QEB50		33.1, 31.9[a]	20.7, 20.0[a]		
73PVP47-*co*-27PMMA35	4.54	54.9	40.1	143	75
73PVP47-*co*-27PMMA35-QEB70		58.8[b]	42.5[b]		

[a] Measured in $CHCl_3$. [b] Measured in H_2O.

The most striking difference between the neutral and ionic cylindrical copolymer brushes is observed by AFM in the dry state as shown in Figures 1 and 2. For the neutral copolymers spin-cast from $CHCl_3$ onto mica wormlike cylinders were observed for both sample 22PVP47-*co*-78PMMA35 (Figure 1a) and sample 73PVP47-*co*-27PMMA35 (Figure 1b). The AFM pictures qualitatively confirm the light scattering results that sample 73PVP47-*co*-27PMMA35 has a significantly higher molar mass than sample 22PVP47-*co*-78PMMA35. From Figure 1a,b the mean length of the cylindrical copolymer brushes, L_n and L_w, may be determined, the values of which are included in Table 3. By comparing the L_w values to the weight-average molar masses, the cylinder length per monomer l is calculated to be 0.17 and 0.15 nm, respectively, the difference being within the experimental error of about ±20%. This is in qualitative agreement with earlier results obtained in solution[9,17] and in the dry state.[7,9]

However, strongly curved structures are found for the respective ionic cylindrical brushes. Figure 2a shows sample 22PVP47-*co*-78PMMA35-QEB50 spin-cast from $CHCl_3$ solution onto mica. Because of the short length of the polymers, mostly "horseshoelike" structures are observed along with some "question marks" for the longer molecules. The hydrophilic sample 73PVP47-*co*-27PMMA35-QEB70 spin-cast from aqueous solution onto mica is shown in Figure 2b. Because of the large contour length of the cylindrical brushes and/or because of the relative side chain lengths of the PVP and PMMA moieties, meanderlike structures are being formed, which seem to exhibit a somewhat smaller curvature radius as compared to sample 22PVP47-*co*-78PMMA35-QEB50 as discussed below

It should be noted that the observed shape change is not correlated with the density of the absorbed molecules at the surface, which depends on subtle effects like the concentration of the solution utilized for spin-casting, the evaporation speed of the solvent, and the polymer/substrate interaction. As concerns the latter point, both the unquaternized and quaternized PVP and PMMA seem to exhibit attractive interactions with mica. A qualitative measure for this interaction is the tendency to obtain single separated molecules at the surface as opposed to monolayer island formation. The latter is a good indication for repulsive interaction, which is almost always observed for polystyrene cylindrical brushes.[8]

The tendency of unquaternized and quaternized PVP as well as of PMMA to adsorb as single chains when spin-cast from various solvents indicates an attractive interaction of all components of the polymer brushes with mica. Thus, a specific solvent effect on the strength of adsorption of the components of the copolymer

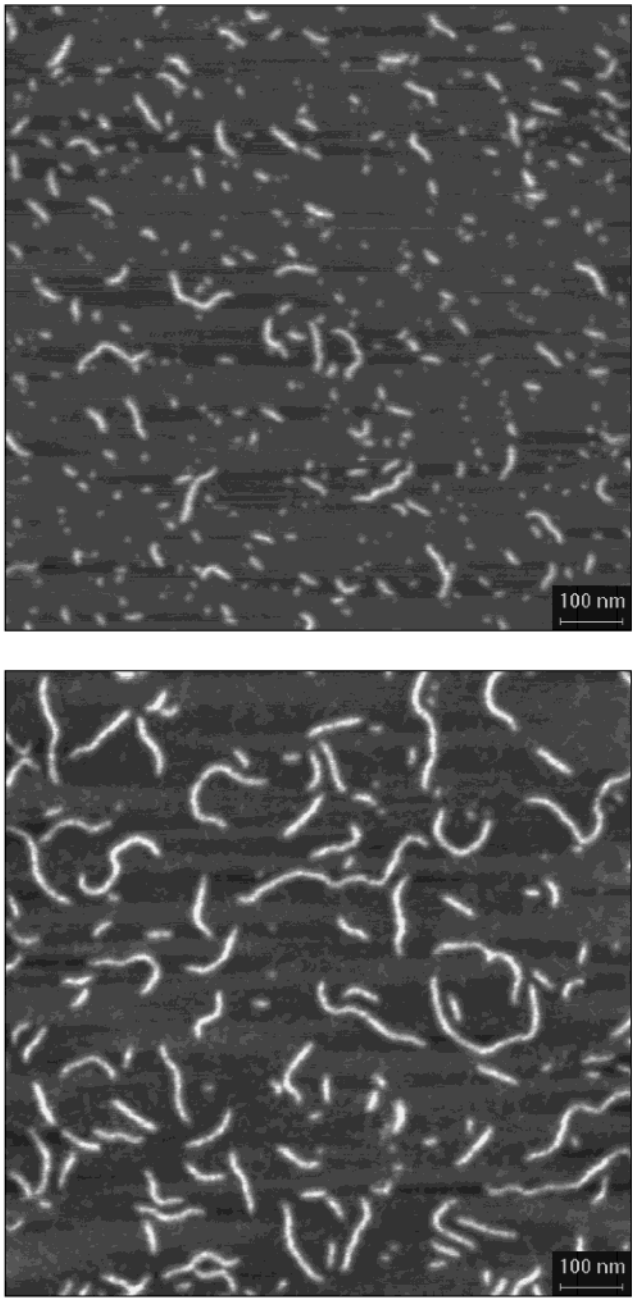

Figure 1. AFM micrograph (height image) of 22PVP47-*co*-78PMMA35 (a, top) and of sample 73PVP47-*co*-27PMMA35 (b, bottom) spin-cast from $CHCl_3$ solution onto mica.

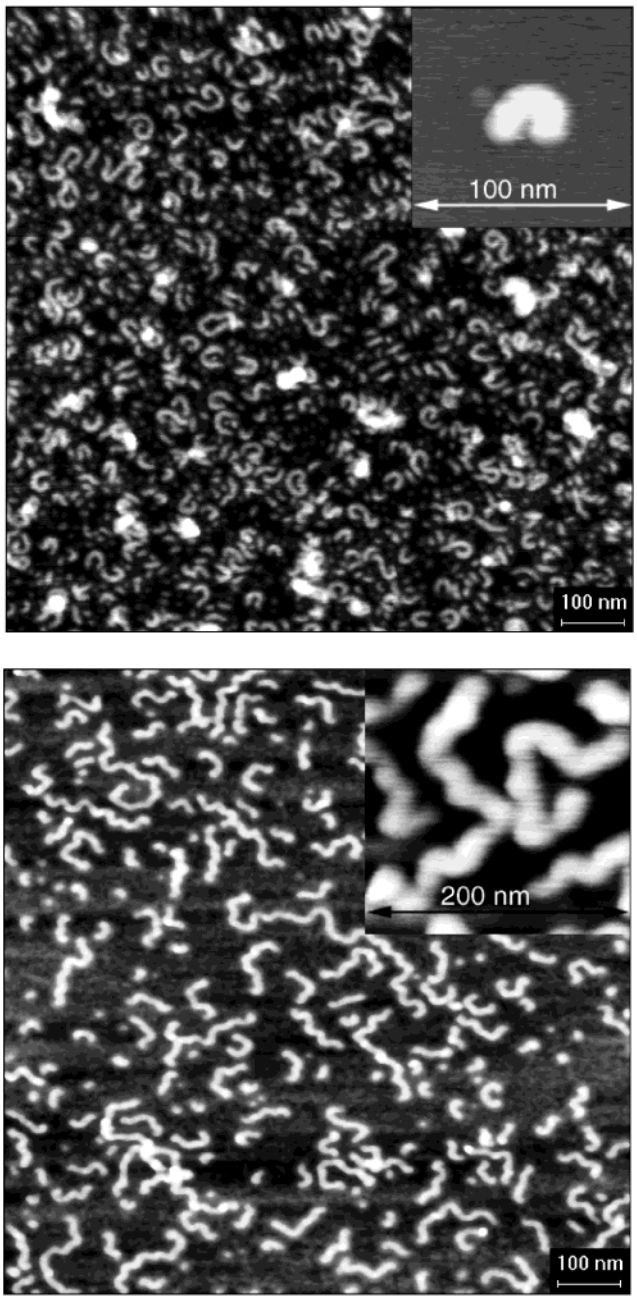

Figure 2. (a, top) AFM micrograph (height image) of 22PVP47-*co*-78PMMA35-QEB50 spin-cast from $CHCl_3$ solution onto mica. The inset shows the magnification of a single horseshoe-shaped brush. (b, bottom) AFM micrograph (height image) of sample 73PVP47-*co*-27PMMA35-QEB70 spin-cast from H_2O solution onto mica. The inset shows the magnification of meandering cylindrical brushes.

brushes is considered to be of minor importance as compared to the selectivity of the solvent leading to chain collapse of the poorly soluble side chains. A quantification of the attractive forces, however, is beyond the scope of the present communication.

The interpretation of the results described above is still a bit vague. The following scenarios could be discussed:

(i) The intramolecular phase separation occurs in dilute solution, and the curvature is induced from the different length, volume, and/or interaction of the PVP and PMMA side chains. However, the light scattering results do not show a shrinking of the molecular dimensions in solution. This means either the phase separation in dilute solution has not yet occurred or the differences in length, volume, and/or interaction of the respective PVP and PMMA side chains is insignificant, i.e., does not represent the driving force for curvature.

Scheme 2. Sketch of Postulated Phase-Separated Side Chains in a Horseshoe Brush (a, top) and in a Meandering Brush (b, bottom)

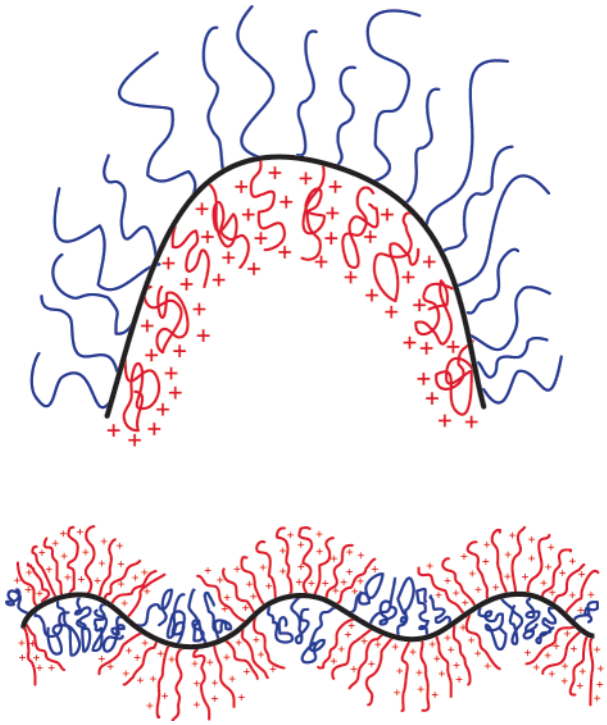

(ii) The intramolecular phase separation occurs during the complex drying process when the polymers are spin-cast from a selective solvent, i.e., a nonsolvent for the minor and a good solvent for the major component. This could be a dynamic, probably nonequilibrium process which comprises collapse and phase separation of the insoluble component followed by drying of the better soluble side chains. This picture is compatible with our experimental results and corroborated by AFM experiments on samples spin-cast from DMF, a good solvent for both side chains. In these pictures only wormlike structures are found similar to those shown in Figure 1 for the unquaternized samples.

(iii) It seems that the curvature of the horseshoe structures is larger than for the meandering cylinders. This could be caused by the larger side chain length of the collapsing PVP chains in sample 22PVP47-*co*-78PMMA-35-QEB50. To prove this hypothesis, more samples with systematically varying side chain length are needed.

On the basis of these observations, we envisage the curved conformations to occur in terms of a local collapse of phase separated nanodomains of the respective minority component as schematically drawn in Scheme 2. For the present experimental system selective solvents are necessary in order to form curved structures. The results in DMF, which show normal wormlike conformations, either suggest that the Flory Huggins interaction parameter is not large enough in order to induce an equilibrium bending as predicted in ref 15 or that the experimental system is more complex than the theoretical model.

Finally, it should be mentioned that peculiar conformations of pure PMMA brushes were observed ranging from spirals[18] to undulations ("buckling")[12] and mean-

derlike structures[19] as well. However, in contrast to the present work, the two latter effects were so subtle that the results varied with the sharpness of the AFM tip. Whereas for each of these structures a theoretical explanation was readily at hand, we are not all convinced that the origin of this structural diversity has been properly understood.

As concerns the present work, the final proof of intramolecular phase separation according to scenario ii can also not be given in the present communication and will be the subject of future investigations. Preliminary attempts to apply electron energy loss spectroscopy (EELS), which principally allows monitoring nitrogen-rich regions with nanometer resolution, failed so far because the sample was evaporated in the electron beam.

Conclusion. Depending on the solvent, statistical copolymer cylindrical brushes adopt different shapes from wormlike to horseshoe or meanderlike structures when spin-cast onto mica. To the best of our knowledge, this is the first time that shape persistent synthetic macromolecules could be chemically manipulated to change their conformation from a wormlike to regularly curved structures. It should be mentioned, though, that for cylindrical brushes with *n*-butyl acrylate side chains a collapse of the wormlike conformation to spherical structures could be induced under pressure on a Langmuir−Blodgett trough.[20] Also, poly(*p*-phenylene)s with amphipolar dendritic side chains were reported to have the potential to intramolecular segregate lengthwise, particularly when spread on a LB trough as well.[21] Our next step will address the question of whether the collapse of the minority component could be detected by scattering experiments in solution, which, however, was not successful so far.

Acknowledgment. Financial support of the DFG and of the Fonds der Chemischen Industrie is gratefully acknowledged.

Supporting Information Available: Description of employed synthesis and characterization techniques. This material is available free of charge via the Internet at http://pubs.acs.org.

References and Notes

(1) Schlüter, A. D. *Top. Curr. Chem.* **1998**, *197*, 165.
(2) Schlüter, A. D.; Rabe, J. P. *Angew. Chem., Int. Ed.* **2000**, *39*, 864.
(3) Gitsov, I. *Adv. Dendritic Macromolecules* **2002**, *5*, 45.
(4) Percec, V.; Ahn, M.; Möller, M.; Sheiko, S. S.; Ungar, G.; Yeardley, D. J. P. *Nature (London)* **1998**, *391*, 161.
(5) Wintermantel, M.; Schmidt, M.; Tsukahara, Y.; Kajiwara, H.; Kohjiya, S. *Makromol. Chem, Rapid Commun.* **1994**, *15*, 279.
(6) Wintermantel, M.; Gerle, M.; Fischer, K.; Schmidt, M.; Wataoka, I.; Urakawa, H.; Kajiwara, K.; Tsukahara, Y. *Macromolecules* **1996**, *29*, 978.
(7) Dziezok, P.; Sheiko, S. S.; Fischer, K.; Schmidt, M.; Möller, M. *Angew. Chem.* **1997**, *109*, 2894.
(8) Sheiko, S. S.; Gerle, M.; Fischer, K.; Schmidt, M.; Möller, M. *Langmuir* **1997**, *13*, 5368.
(9) Gerle, M.; Fischer, K.; Roos, S.; Müller, A. H. E.; Schmidt, M.; Sheiko, S. S.; Prokhorova, S.; Möller, M. *Macromolecules* **1999**, *32*, 2629.
(10) Kawaguchi, S.; Mauiruzzaman, M.; Katsuragi, K.; Matsumato, H.; Ito, K.; Hugenberg, N.; Schmidt, M. *Polym. J.* **2002**, *34*, 253.
(11) Shu, L.; Schlüter, D.; Ecker, S.; Severin, N.; Rabe, J. P. *Angew. Chem., Int. Ed.* **2001**, *40*, 4666.
(12) Sheiko, S. S.; Möller, M. *Top. Curr. Chem.* **2001**, *212*, 138.
(13) Saariaho, M.; Subbotin, A.; Szleifer, I.; Ikkala, O.; ten Brinke, G. *Macromolecules* **1999**, *32*, 4439.
(14) Saariaho, M.; Subbotin, A.; Ikkala, O.; ten Brinke, G. *Macromol. Rapid Commun.* **2000**, *21*, 110.
(15) Stepanyan, R.; Subbotin, A.; ten Brinke, G. *Macromolecules* **2002**, *35*, 5640.
(16) Our preliminary attempt to copolymerize polystyrene and PVP macromonomers in benzene failed because shortly after the initiation macroscopic phase separation occurred in the reaction mixture.
(17) Fischer, K.; Schmidt, M. *Macromol. Rapid Commun.* **2001**, *22*, 789.
(18) Khalatur, P. C.; Khokhlov, A. R.; Prokhorova, S. A.; Sheiko, S. S.; Möller, M.; Shirvanyanz, D. G.; Starovoitova, N. *Eur. Phys. J. E* **2000**, *1*, 99.
(19) Sheiko, S S.; Borisov, O. V.; Prokhorova, S. A.; Möller, M. Manuscript in preparation.
(20) Sheiko, S. S.; Prokhorova, S. A.; Baers, K. L.; Matyjaszewski, K.; Patemkin, I. I.; Khokhlov, A. R.; Möller, M. *Macromolecules* **2001**, *34*, 8354.
(21) Bo, Z.; Rabe, J. P.; Schlüter, A. D. *Angew. Chem., Int. Ed.* **1999**, *38*, 2379.

MA025711R